

Enhancement of the Cytotoxic Effect of Anticancer Agent by Cytochrome c Functionalised Hybrid Nanoparticles in Hepatocellular Cancer Cells

Abstract

Treatment of hepatocellular cancer with chemotherapeutic agents has limited success in clinical practice and their efficient IC_{50} concentration would require extremely high doses of drug administration which could not be tolerated due to systemic side effects. In order to potentiate the efficacy of anticancer agents we explored the potential of co-treatment with pro-apoptotic Cytochrome c which activates the apoptotic pathway downstream of p53 that is frequently mutated in cancer. To this end we used hybrid iron oxide-gold nanoparticles as a drug delivery system to facilitate the internalisation of Cytochrome c into cultured HepG2 hepatocellular carcinoma cells. Our results showed that Cytochrome c can be easily conjugated to the gold shell of the nanoparticles which are readily taken up by the cells. We used Cytochrome c in concentration ($0.2\mu\text{g mL}^{-1}$) below the threshold required to induce apoptosis on its own. When the conjugate was administered to cells treated by doxorubicin, it significantly reduced its IC_{50} concentration from $9\mu\text{g mL}^{-1}$ to $3.5\mu\text{g mL}^{-1}$ as detected by cell viability assay, and the efficiency of doxorubicin on decreasing viability of HepG2 cells was significantly enhanced in the lower concentration range between $0.01\mu\text{g mL}^{-1}$ to $5\mu\text{g mL}^{-1}$. The results demonstrate the potential of the application of therapeutic proteins in activating the apoptotic pathway to complement conventional chemotherapy to increase its efficacy. The application of hybrid iron oxide-gold nanoparticles can also augment the specificity of drug targeting and could serve as a model drug delivery system for pro-apoptotic protein targeting and delivery.

Keywords

Hepatocellular cancer; Chemotherapy; Doxorubicin; Apoptosis; Cytochrome c; Hybrid nanoparticles; Drug delivery system

Research Article

Volume 1 Issue 2 - 2014

**Maryam Malekigorji, Clare Hoskins,
Tony Curtis and Gabor Varbiro***

*School of Pharmacy, Institute of Science and Technology in
Medicine, Keele University, UK*

***Corresponding author:** Gabor Varbiro, Institute of
Science and Technology in Medicine, Keele University,
Keele, Staffordshire, UK, Tel: +441782 733877; E-mail:
g.varbiro@keele.ac.uk

Received: November 13, 2014 | **Published:** November
22, 2014

Abbreviations

HCC: Hepato Cellular Cancer; GNPs: Gold Nanoparticles; HNP: Iron oxide gold Nanoparticles; MRI: Magnetic Resonance Imager

Introduction

Hepatocellular cancer (HCC) is the sixth most common type of cancer and the third in cancer-associated death. It has been traditionally managed by either surgical intervention [1] or by other approaches such as transcatheter arterial tumor chemoembolization, drug-eluting bead embolization and radiofrequency ablation [2], while the systemic anticancer therapy of HCC is limited to a few drugs including, doxorubicin or paclitaxel [3-4]. Their clinical efficacy however has not been verified by controlled clinical trials. A moderate increase in the median overall survival rate has recently been demonstrated using multikinase inhibitor - sorafenib [5], but an effective therapy for HCC is currently considered to be a significant unmet medical need [6].

Programmed cell death is frequently associated with cancer. Defects in the apoptotic pathway may contribute to the onset of cancer since cell growth is unchecked in the presence of an oncogenic signal [7]. Therefore the activation of programmed

cell death could be an ideal solution for controlling and reducing tumor volume [8]. Numerous proteins are involved in apoptosis and thus serve as both potential targets as well as therapeutic tools in cancer treatment. A crucial event during apoptosis is the release of intra-mitochondrial pro-apoptotic proteins into the cytosol, which marks the point of no return in the process [9]. One of the proteins translocated from the mitochondria to the cytosol is Cytochrome c (Cyt c), a 12.7 kDa protein that is also involved in the transport of electrons in the mitochondrial respiratory chain, shuttling electrons between respiratory complex III and IV [10]. Following an apoptotic stimuli, Cyt c released from the mitochondria facilitates the assembly of the apoptosome which comprises of apoptosis activating factor 1 (Apaf-1), pro-caspase 9 and dATP and initiates the activation of the caspase cascade [11]. This mechanism can be exploited in practice by introducing Cyt c into tumor cells which can trigger apoptosis and lead to cell death. However, the intracellular targeting of proteins exhibits significant challenges and it requires the application of specific drug delivery systems.

There have previously been attempts to introduce Cyt c into cells using lipid-apolipoprotein particles [12], biodegradable chimeric polymersomes [13], mesoporous silica nanoparticles with a pore surface that undergoes charge conversion intracellularly [14], biodegradable polymersomes containing

an ionisable membrane [15], protein encapsulating theranostic nanoparticles [16] or Cyt c based protein nanoparticles [17]. The external delivery of Cyt c was also demonstrated to activate the apoptotic pathway in HeLa cells [17-18]. The target specificity nanoparticles containing Cyt c can be enhanced by utilizing folate receptors for active targeting [16]. A wide range of tumors over express folate receptors on their surface and their ligand, folic acid, can be conjugated to the nanoparticles to enhance the targetability of the attached compounds and thereby increase their therapeutic efficiency [19].

Gold nanoparticles (GNPs) have been previously used to conjugate Cyt c [20]. Hybrid iron oxide-gold nanoparticles (HNPs) are composed of an iron oxide core surrounded by a rigid gold shell. These particles can undergo manipulation via external stimulus due to the inherent magnetism of the iron oxide core [21]. The magnetic qualities result in the ability to image these particles using a magnetic resonance imager (MRI), whilst the gold shell renders the particles biocompatible and easily functionalised. These factors result in a more precise therapy leading to decreased patient side effects. Hybrid nanoparticles have previously been shown to be effective vehicles for the delivery of anticancer agents in pancreatic cancer cells [22]. Cytotoxic agent 6-thioguanine was conjugated directly onto the HNP via dative covalent linkage between the thiol (-SH) moiety in the drug compound and the gold surface. After exposure to human pancreatic adenocarcinoma cells (BxPC-3) the IC_{50} was reduced 10-fold using the HNP-6TG conjugate compared with the free drug. Drug uptake studies showed that after conjugation to the HNP, increased intracellular concentrations of 6-TG were observed compared with the free drug. This data highlights the potential of HNPs as delivery vehicles of pharmaceutical cargo enabling enhanced cellular internalisation hence increasing drug efficiency [22]. Pro-apoptotic proteins, such as Cyt c, can be administered to complement anticancer drugs and thus enhance their effect. In this case the simultaneous administration of pro-apoptotic proteins with anticancer agents can induce cell death in tumor cells while the dose of the antineoplastic drugs required for this therapeutic effect could be decreased. This subsequently reduces the severity of side effects without compromising the therapeutic efficacy of the cytotoxic compounds. In this study we evaluated the co-administration of the anticancer agent doxorubicin with Cyt c conjugated HNPs in liver cancer cells to demonstrate the potentiating pharmacological action and quantify the alteration of IC_{50} value of doxorubicin co-administered with Cyt c in cultured liver cancer cells.

Materials and methods

Materials

Doxorubicin was from LC Laboratories (Woburn, MA, USA); Bovine Cytochrome c and all other compounds were from Sigma-Aldrich (Gillingham, UK) unless otherwise stated. HepG-2 human hepatocellular carcinoma cell line was from American Type Culture Collection (Manassas, VA, USA). The cell line was grown in humidified 5% CO_2 atmosphere at 37°C and maintained in culture as monolayer adherent cells in Dulbecco's Modified

Eagle's Medium containing 1% penicillin-streptomycin solution (Sigma) and 10% foetal calf serum (FSC). Cells were passaged at intervals of 3 days.

Synthesis and characterisation of hybrid nanoparticles

Hybrid nanoparticles were prepared as previously described [21,22]. Briefly, iron oxide nanoparticles were synthesized via wet chemical precipitation methods. These negatively charged particles were electrostatically coated with poly (ethylenimine) MW 200,000. Gold seeds (2 nm) were prepared via reduction of $H AuCl_4$ and electrostatically attached onto the polymer coated iron oxide. Iterative reduction of the acidic gold rendered complete gold coating. The particles were characterised by zeta potential measurement (Zetasizer Nano-ZS, Malvern Instruments, UK), inductively coupled plasma-optical emission spectroscopy (Agilent, UK), transmission electron microscopy (JEOL JEM-1230, JEOL, Japan) and UV-Vis spectroscopy (UV-2600 UV-VIS(NIR) with an ISR-2600 Plus Integrated sphere, Shimadzu, Germany).

Protein conjugation and quantification

Protein conjugation was carried out stirring Cyt c (25 mg) with the HNPs (5 mL, 5 $mg mL^{-1}$) at room temperature for 3 h. Addition of O-[2-(3-Mercaptopropionyl amino) ethyl]-O'-methylpolyethylene glycol (PEG-Thiol) onto the HNP-c structure was achieved by adding 12.5 mg into the HNP solution in parallel with Cytochrome c. The particles were magnetically separated from solution and washed thoroughly with deionised water five times. The particles were resuspended in 5 mL deionised water to a final concentration of 5 $mg mL^{-1}$ (Fe) which was confirmed using ICP-OES (data not shown). UV-Vis spectrometry was used to quantify the drug concentration conjugated to the particle surface (HNP-c). The absorbance was measured at 410 nm on a UV-2600 UV-VIS(NIR) with an ISR-2600 Plus Integrated sphere (Shimadzu, Germany), and compared with a calibration curve ($R^2 = 0.999$).

Cellular uptake of Cytochrome c

HepG2 cells (3 mL) in exponential growth phase were seeded into 6-well plates and incubated for 24 h at 37°C with 5% CO_2 . The media was replaced with Cyt c, HNP-c and HNP-c-PEG (50 or 100 $\mu g mL^{-1}$) and incubated for 1 and 4 h. The medium was removed and each well was washed with PBS before adding trypsin into each well. Cells were resuspended in 1 mL media and viable cells were counted using an automated cell counter (Invitrogen countess, UK). Cells (100,000) were transferred into Eppendorf tubes and centrifuged (800 rpm for 5 min). The supernatant was removed and cells were resuspended in 1 mL water. Cyt c concentration was analysed using UV/Vis spectrometry (UV-2600 UV-VIS (NIR) with an ISR-2600 plus Integrated sphere, Shimadzu, Germany) at 410 nm and calculated per cell.

Cellular imaging

Intracellular imaging using TEM: Cellular internalisation images were taken after incubation of HNPs with HepG-2 cells. Cells were grown into Aclar slides and incubated with HNP (25 $\mu g mL^{-1}$, 24 h). Cells were washed with PBS and fixed with 2.5%

glutaraldehyde in 0.1 M sodium cacodylate buffer: 2 mM calcium chloride (50:50) for 2 h. The samples were washed for 5 mins in 0.1 M sodium cacodylate buffer: 2 mM calcium chloride and this step were repeated a further two times. The samples were post fixed in 0.1 % osmium tetroxide in 0.1 M sodium cacodylate buffer / 2 mM calcium chloride for 1 h. Serial dehydrations was carried out in ethanol before the samples were embedded in spur resin. The samples were sectioned using a freshly cut diamond knife and placed onto formvar coated copper grids for imaging. The samples were imaged using JEOL JEM-1230 microscope (Jeol, Japan) using Analysis software.

Imaging of cellular interactions with formulations using atomic force microscopy: HepG2 cells were seeded in 6-well plates containing glass coverslips. Cells were incubated for 24 h at 37°C and 5 % CO₂. After 24 h the media was replaced with doxorubicin, Cyt c, HNP-c, HNP-c-PEG, combination of HNP-c-PEG and doxorubicin (25 µgmL⁻¹) and further incubated for 1 and 4 h. After abundant washing with PBS cells were fixed with 2.5% glutaraldehyde in PBS for 10 min. Fixed cells were washed 5 times with PBS and mounted on glass slides. Cell topography was imaged using a Bruker Catalyst Atomic Force Microscope (Bruker, Germany) using Peak Force Tapping Mode and a ScanAsyst in air cantilever.

Cell viability assay

HepG2 cells were seeded into 96-well plates at a starting density of 15,000 cells per well and cultured overnight in humidified 5% CO₂ atmosphere at 37°C. After 24 h, doxorubicin and/ or HNP- c at the indicated concentrations were added to the medium. After 24 h, 0.5% of the water-soluble mitochondrial dye 3-(4,5-dimethyl-2-thiazolyl)-2,5-diphenyl-2H-tetrazolium bromide (MTT⁺) was added. Incubation was continued for three more hours, the medium was removed and the water-insoluble blue formazan dye formed stoichiometrically from MTT⁺ was solubilized by acidic SDS. Optical densities were determined by a microplate reader (Tecan Infinite 200 Pro, Austria) at the wavelength of 570 nm.

Trypan blue assay

HepG2 cells in exponential growth phase were seeded into 12-well flat bottomed plates at a starting density of 500,000 cells / well and incubated for 24 h at 37°C with 5 % CO₂. The media was replaced with doxorubicin and / or HNP-c at various concentrations as indicated. Cells were incubated for 24 h, subsequently the media was removed and cells were washed 3 times with PBS. The cells were trypsinised and resuspended in fresh media. A mixture of 50 µL of cells and 50 µL of trypan blue solution was placed in an automated cell counter (Invitrogen countess, UK) and viable cells were counted. The percentage viability was calculated in relation to control cells.

Statistical Analysis

The IC₅₀ values were calculated by Graph Pad Prism 6 software. Data were presented as means ± S.E.M. For multiple comparisons of groups, ANOVA was used. Statistical difference between groups was established by paired or unpaired Student's t test, with Bonferroni correction.

Results

Characterisation of hybrid nanoparticles

The hybrid nanoparticle step by step synthesis was monitored by zeta potential measurement (Figure 1A). The shift in gold maximum absorbance spectra from 520 nm of the gold seeds to 600 nm confirmed the coating had been successful (Figure 1B). TEM confirmed the morphology and size of the HNPs (Figure 1C). The metal content of the particles was determined to be 3.65 mgmL⁻¹: 0.68 mgmL⁻¹ Fe: Au respectively. All further concentrations relating to the HNPs will be due to the Fe content.

Protein conjugation and quantification

Cytochrome c attachment was quantified using UV/Vis spectroscopy. The concentration of Cyt c attached to the HNP and HNP-PEG formulation were 1.64 mgmL⁻¹ and 1.37 mgmL⁻¹ respectively (Table 1). The reduced difference Cyt c concentration attached to the PEGylated HNP may be due to the PEG-thiol competing with the Cyt c for binding space on the gold surface. The UV-Vis spectra (Figure 2) showed that before Cyt c conjugation, the HNPs did not absorb in the region of 410 nm (λ_{max} for Cyt c). However, after protein conjugation both the PEGylated and unPEGylated conjugates absorbed at this wavelength.

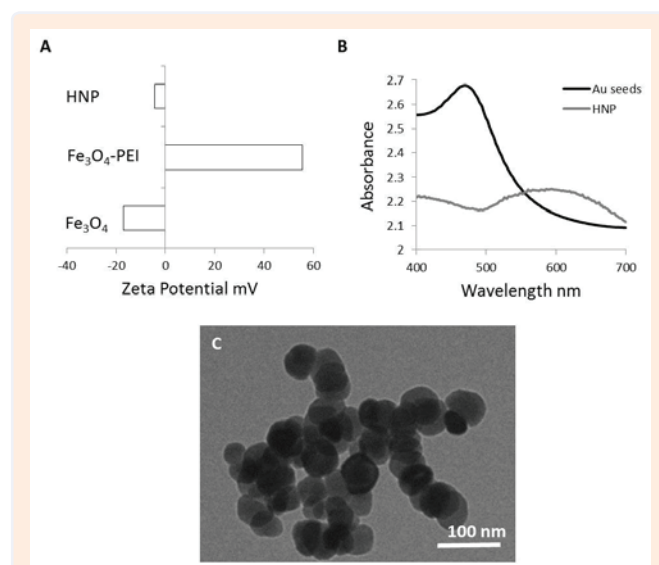


Figure 1: Characterization of hybrid nanoparticles using
A) Zeta potential measurement
B) UV-Vis spectroscopy
C) TEM microscopy

Table 1: Concentration of Cyt-c in HNP and HNP-PEG formulation determined by ICP and UV/Vis.

Samples	Concentration mgmL ⁻¹		
	Fe	Au	Cytochrome c
HNP	2.653	0.6827	-
HNP-c	1.00	0.2573	2.586
HNP-c-PEG	1.00	0.2573	2.082

Cellular uptake of Cytochrome c

In order to demonstrate that Cyt c has been delivered into the cultured hepatocytes, the cellular uptake of Cyt c either alone or attached to HNP and HNP-PEG particles was assessed. UV-Vis spectroscopy showed that cellular uptake depended on the loading concentration rather than time (Figure 3). The intracellular level of Cyt c did not show any significant alteration when cells were incubated with 0.2 mgmL⁻¹ or 0.5 mgmL⁻¹ of Cyt c alone. In contrast to this, when Cyt c was conjugated to HNP or HNP-PEG the drug uptake was significantly higher ($p < 0.05$) when compared to incubation with Cyt c alone (Figure 2). No difference was observed in the cellular when cells were incubated with Cyt c conjugated to either HNP or HNP-PEG (Figure 3). These findings suggest that after greater cellular uptake can be achieved after HNP attachment. This is possibly through entry via endocytosis which may not be the route of entry of the free drug.

Cellular imaging

The internalisation of HNP into HepG2 cells was verified by transmission electron microscopy (Figure 4). The TEM micrograph shows the presence of the HNPs inside the cellular membrane. These are proposed to have been internalised via endocytosis. The image verifies that the whole HNP-c (PEG and non-PEG) formulation enters the cell and this compliments the rationale that HNP attachment results in greater cellular uptake. Atomic force microscopy was used to demonstrate cellular response following incubation with nanoparticles (Figure 5A-5D). The images obtained show the cellular topography which can give an indication of the state of the cell. In agreement with the Cyt c uptake study the HNP bound particles (Figure 3) appear to be differing in shape and roughness to the control cells and Cyt c. This would suggest that after incubation of the HNP formulations, the increased level on Cyt c entering the cell is enough to initiate a cellular response and the start of cellular destruction. A control sample using HNPs with no Cyt c was also imaged which showed no deviation from the control cells (data not shown).

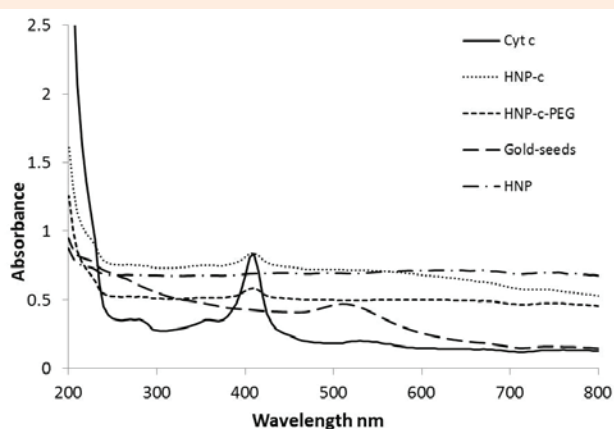


Figure 2: UV-Vis spectra confirming protein attachment onto the HNP surface evidenced by absorption at 410 nm.

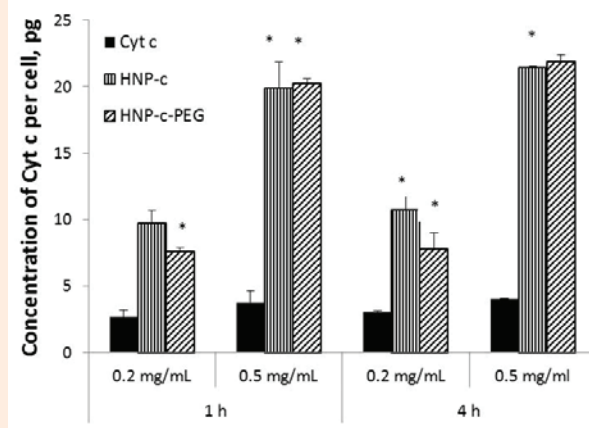


Figure 3: Quantification of intracellular Cyt c concentration in HepG2 cells after incubation with Cyt c and HNP formulations over 1 and 4 h ($n = 3 \pm \text{SEM}$)

*: significant difference ($p < 0.05$) between HNP-c or HNP-c-PEG and Cyt-c by paired t test

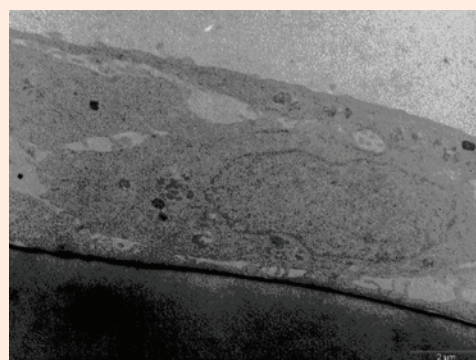


Figure 4: TEM micrograph of HepG2 cells with HNPs internalized within their structure.

Determining the effect of Cytochrome c, HNP-c and HNP-c-PEG on cell viability

MTT⁺ assay was used to assess the effect of, Cyt c, HNP conjugated with Cyt c (HNP-c) and the PEGylated counterpart (HNP-c-PEG) on cell viability (Figure 6). Cyt c alone induced a moderate decrease in cell viability as demonstrated by MTT⁺ assay. When cells were incubated with HNP-c the decrease in cell viability was significantly larger ($p < 0.05$) at or above the concentration of 10 $\mu\text{g mL}^{-1}$. When cells were incubated with HNP-c-PEG the decrease in cell viability was significantly larger ($p < 0.05$) at or above the concentration of 5 $\mu\text{g mL}^{-1}$ (Figure 5). HNP-c-PEG was found to be more potent in decreasing the viability of HepG2 cells than HNP-c possibly due to the PEG moiety allowing increased entry into the cell (in agreement with the cellular uptake assay (Figure 3) however the difference was not found to be significant. At the concentrations tested, no IC₅₀ was evident for the free Cyt c protein. The 50% decrease in cell viability was noticed with HNP-c or HNP-c-PEG at the concentration of approximately 2×10^{-1} mgmL⁻¹ which is in line

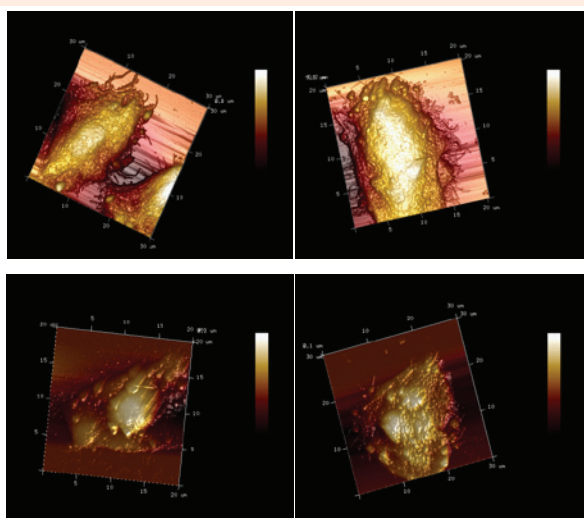


Figure 5: AFM image of HepG2 cells after 1 hr incubation with.
 A) Control cells
 B) Cells with 25 µg_{mL}⁻¹ of HNP
 C) Cells with 25 µg_{mL}⁻¹ of Cyt c
 D) Cells with 25 µg_{mL}⁻¹ of HNP-c-PEG

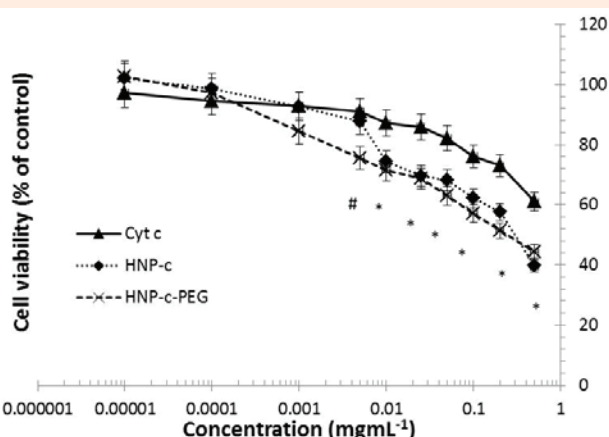


Figure 6: Effect of Cyt-c, HNP-c and HNP-c-PEG on viability of cells. The effect of Cyt-c, HNP-c and HNP-c-PEG on viability of HepG2 cells was detected by the formation of water-insoluble blue formazan dye from the yellow mitochondrial dye MTT⁺ by the functionally active mitochondria of the cells. The cells were exposed to different concentrations of Cyt-c, HNP-c and HNP-c-PEG for 24 h before the addition of the MTT⁺ dye. Data represent average ± S.E.M. of three independent experiments.
 *: significant difference ($p < 0.05$) between HNP-c or HNP-c-PEG and Cyt-c; #: significant difference ($p < 0.05$) between HNP-c-PEG and Cyt-c by paired t test

with previously reported results [18,23], which found the IC_{50} of Cyt c to be 3.5×10^{-1} mg_{mL}⁻¹.

Cell viability was also determined by trypan blue dye exclusion test to ensure that the Cyt c introduced into HepG2 cells do not interfere with the mitochondrial respiration and thus bias the MTT⁺ assay. Therefore, HepG2 cells were again incubated

with Cyt c, HNP-c and HNP-c-PEG for 24 h in the concentration range between 10^{-5} and 5×10^{-1} mg_{mL}⁻¹ and cell viability was expressed as the percent of controls (Figure 7). Cyt c alone induced a moderate decrease in cell viability as demonstrated by trypan blue assay. When cells were incubated with HNP-c-PEG, the decrease in cell viability was significantly larger ($p < 0.05$) at or above the concentration of 5 µg_{mL}⁻¹ when compared to Cyt-c alone. When cells were incubated with HNP-c the decrease in cell viability was significantly larger ($p < 0.05$) at or above the concentration of 0.1 µg_{mL}⁻¹ (Figure 7) when compared to Cyt-c alone. HNP-c was found to be more potent in decreasing the viability of HepG2 cells than HNP-c-PEG as demonstrated by trypan blue dye exclusion test; however no significant difference was found between their effects at or above the concentration of 5 µg_{mL}⁻¹ (Figure 7). In agreement with the MTT⁺ assay, no IC_{50} was evident over the concentrations tested. In order to evaluate if the co-administration of Cyt-c enhances the cytotoxic effect of doxorubicin, we used the concentration of HNP-c-PEG that decreased the viability by 10% which was 0.2 µg_{mL}⁻¹.

Determining the effect of doxorubicin, and doxorubicin plus HNP-c-PEG on cell viability

MTT⁺ assay was used to assess the effect of doxorubicin and doxorubicin plus HNP-c-PEG on cell viability (Figure 8). Doxorubicin alone induced a marked decrease in cell viability as demonstrated by MTT⁺ assay with the IC_{50} value of 9 µg_{mL}⁻¹ (Table 2). When varying concentration of doxorubicin was co-administered with HNP-c-PEG at the concentration of 0.2 µg_{mL}⁻¹ there was a significant decrease ($p < 0.05$) in cell viability in the lower concentration range from 0.01 µg_{mL}⁻¹ to 5 µg_{mL}⁻¹ (Figure 8). The IC_{50} value of doxorubicin plus HNP-c-PEG was also significantly reduced from 9 µg_{mL}⁻¹ to 3.5 µg_{mL}⁻¹ (Table 2).

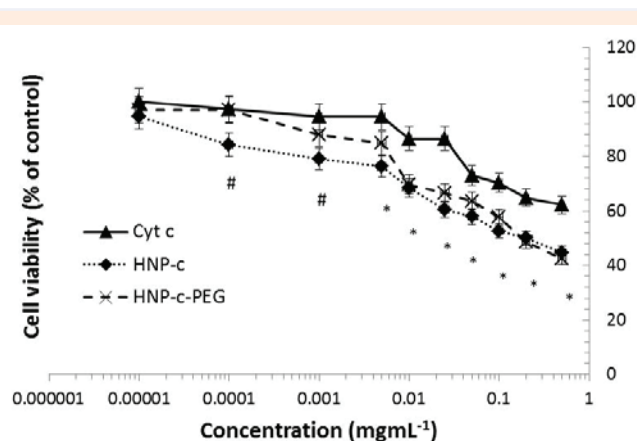


Figure 7: Effect of Cyt-c, HNP-c and HNP-c-PEG on viability of cells. The effect of Cyt-c, HNP-c and HNP-c-PEG on viability of HepG2 cells was detected by trypan blue dye exclusion test. The cells were exposed to different concentrations of Cyt-c, HNP-c and HNP-c-PEG for 24 h before the addition of the trypan blue dye. Data represent average ± S.E.M. of three independent experiments. *: significant difference ($p < 0.05$) between HNP-c or HNP-c-PEG and Cyt-c; #: significant difference ($p < 0.05$) between HNP-c and Cyt-c by paired t test

When doxorubicin was administered at concentrations higher than $5 \mu\text{g mL}^{-1}$, the co-administration of $0.2 \mu\text{g mL}^{-1}$ HNP-c-PEG did not enhance further the effect of doxorubicin on the cell viability detected by MTT⁺ assay (Figure 8). The co-administration of doxorubicin with $0.2 \mu\text{g mL}^{-1}$ HNP-PEG (nanoparticles not containing Cyt c) did not enhance the effect of doxorubicin on the cell viability, nor did it facilitate any alteration in its IC₅₀ value (data not shown).

Cell viability was also determined by trypan blue dye exclusion test to ensure that the Cyt c co-administered with doxorubicin into HepG2 cells do not interfere with the mitochondrial respiration and thus bias the MTT⁺ assay. In this case HepG2 cells were again incubated with doxorubicin and doxorubicin plus HNP-c-PEG in the same concentration as described above. The viability of HepG2 cells did not show any alteration regardless of it being assessed by MTT⁺ assay or by trypan blue dye exclusion test (data not shown).

Discussion

The common approach in cancer chemotherapy involves

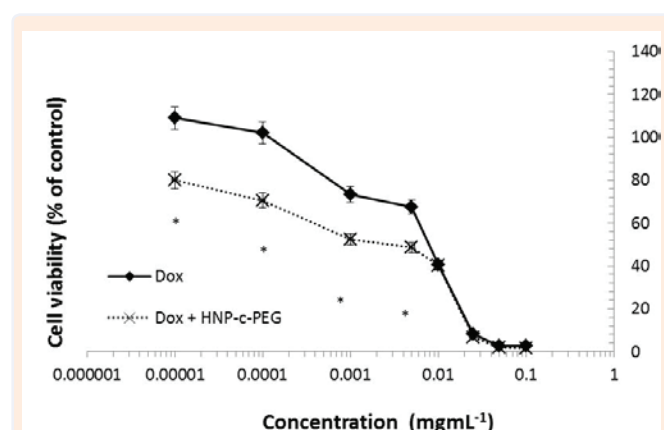


Figure 8: Effect of Doxorubicin, Doxorubicin plus HNP-c-PEG on viability of cells.

The effect of Doxorubicin or Doxorubicin plus HNP-c-PEG on viability of HepG2 cells was detected by the formation of water-insoluble blue formazan dye from the yellow mitochondrial dye MTT⁺ by the functionally active mitochondria of the cells. The cells were exposed to different concentrations of Doxorubicin or Doxorubicin plus HNP-c-PEG for 24 h before the addition of the MTT⁺ dye. Data represent average \pm S.E.M. of three independent experiments.

*: significant difference ($p < 0.05$) between Doxorubicin and Doxorubicin plus HNP-c-PEG by paired t test

Table 2: The IC₅₀ values of the drugs and formulation determined by MTT⁺ and trypan blue assay in HepG2 cells.

Samples	IC ₅₀ from MTT ⁺ assay ($\mu\text{g mL}^{-1}$)	IC ₅₀ from trypan blue assay ($\mu\text{g mL}^{-1}$)
Cyt c	-	-
HNP-c	28	20
HNP-c-PEG	24	18
Doxorubicin	9	8
Doxorubicin + HNP-c-PEG	3.5	3
HNP	-	-

the systemic administration of various cytotoxic drugs that do not have tumor specificity [24]. Since they also affect normal cells leading to undesired side effects, this often limits their therapeutic application. There have been numerous efforts to enhance the efficacy of cancer therapy. This is particularly true for HCC, because there is hardly any therapeutic approach which exhibits significant clinical benefits. Anticancer agents can exert their effect by different mechanisms of action (like inhibiting enzymes or targeting receptors) and can be divided into main categories such as cytotoxic drugs, hormones, monoclonal antibodies or protein kinase inhibitors [25]. The common principle of all anticancer agents is that they ultimately activate the programmed cell death pathway, leading to the death and elimination of target cells. This however requires the involvement of the p53-dependent apoptotic pathway which is frequently mutated in a large number of cancers and provides an explanation why p53-mutated cancers respond poorly to anticancer agents [26]. Activating a p53 independent apoptotic pathway for therapy is a possible route by which an efficient cancer treatment can be established. Cyt c, a crucial mediator of apoptosis released from the mitochondria, acts downstream of p53 in the apoptotic pathway and activates the effector caspases making the programmed cell death process irreversible. Therefore the intracellular delivery of Cyt c could activate the programmed cell death pathway even if the upstream processes are dysfunctional.

Cyt c is a protein with a molecular weight of 12.7kDa which makes the intracellular delivery particularly challenging. The stability of protein pharmaceuticals is limited and their physical and chemical properties make them unfavourable drug candidates [27]. Due to its size, Cyt c does not readily cross the membrane bilayer and requires the development of an efficient drug delivery system that allows sufficient levels of drug to be delivered into the Cytoplasm to exert a therapeutic effect. The intracellular delivery of Cyt c has been attempted previously in numerous ways such as direct delivery following electroporation [23], or nanoprecipitated to form protein nanoparticles which were subsequently surface coated with poly (lactic-co-glycolic) acid, which when taken up by HeLa cells resulted in caspase-dependent apoptosis [17]. Other reports showed direct attachment of Cyt c onto the surface of different types of nanoparticles. These include nanoparticles such as gold [28,29], silica [30] and polymers [17] functionalised with Cyt c. While these studies have shown great potential in delivery of the protein and activation of the caspase pathway, real time tracking is not always possible. The advantage of HNP-c is the multifunctional ability of these particles to be both protein carrier vehicles as well as imaging agents.

Cyt c conjugation to HNPs was confirmed by UV-Vis spectroscopy (Figure 2), and 40% or 50% of the loading concentration of Cyt c was shown to be attached to the HNP in the presence or absence of PEG on the nanoparticle surface, respectively (Table 1). The HNP-c-PEG particles were internalized into HepG2 cells presumably by endocytosis and their intracellular concentration was also quantified (Figure 3). Cellular uptake of Cyt c attached to HNPs into HepG2 cells was

significantly higher when compared to free Cyt c. The loading concentration – but not the period of incubation – influenced the cellular uptake of Cyt c; incubation with higher concentration (0.5 mgmL^{-1} vs. 0.2 mgmL^{-1}) resulted in a two to three fold increase in the intracellular concentration of Cyt c (Figure 3) This suggests that the uptake is possibly driven by a concentration gradient further supporting the theory that HNP internalisation is by endocytosis. The internalized HNPs in HepG2 cells were demonstrated by TEM (Figure 4) and by atomic force microscopy (Figure 5) respectively.

The effect of Cyt c on decreasing the viability of HepG2 cells was noticeable from the concentration of $5 \mu\text{gmL}^{-1}$ or higher (Figure 6). In order to verify that the co-administration of Cyt c with doxorubicin enhances the effect of the later on cell viability, we choose a concentration of HNP-c-PEG that corresponds to only a 10% decrease in cell viability. This amount of HNP-c-PEG ($0.2 \mu\text{gmL}^{-1}$) did not enhance the natural cytotoxicity of the nanoparticles and was deemed ideal to be used together with varying concentration of the anticancer agent. While there were previous studies showing the apoptosis inducing effect of internalized Cyt c, the reported work aimed to demonstrate that if a low level of the pro-apoptotic protein – which itself does not activate the programmed cell death pathway – can enhance the effect of a conventional anticancer agent, such as doxorubicin. Furthermore, the concentration of Cyt c used in our experiments was 10 to 100 fold lower than that reported by others. Our results showed a marked decrease of the IC_{50} of doxorubicin from $9 \mu\text{gmL}^{-1}$ to $3.5 \mu\text{gmL}^{-1}$ and the efficiency of the combination was particularly noticeable in the low concentration range (Figure 8).

Cyt c is an electron carrier in the mitochondrial respiratory chain, and since the MTT^+ assay is also associated with mitochondrial oxidative phosphorylation, in order to verify that the external Cyt c does not interfere with this process, another method was also applied to assess the cell viability. The results from both methods were similar (Table 2), showing that the intracellular delivery of Cyt c enhances the efficiency of doxorubicin. Furthermore the enhancement of doxorubicin-induced cell death by Cyt c was synergistic; the resulting decrease in viability was larger than the sum of their separate effects on viability. This phenomenon is particularly important from the aspect of HCC, since no efficient chemotherapy is available for the treatment, which is exceptionally concerning when a tumor is found to be surgically inoperable [2].

The delivery of therapeutic proteins in general and particularly those that can exert their effect in the absence of a function p53 are promising experimental therapeutic modalities for incurable and / or drug resistant cancers. However therapeutic proteins have limited physical and chemical stability, are easily degradable and have a short plasma half-life. It is therefore essential to develop a drug delivery system that can efficiently deliver its load to the target and protect the attached proteins from degradation. A further challenge is the effective targeting of the therapeutic proteins. This can be addressed by coating the surface of nanoparticles with ligands which bind to receptors abundant in the membrane of cancer cells and thus facilitate the

internalisation of the attached therapeutic protein. An example is folate since a wide range of tumors over express folate receptors on their surface [16]. Liver cancers over express the glucose-regulated protein 78 receptors on their surface which can be targeted by highly specific Pep42 motif and since it does not exert any toxic effect, hence it can be a safe HCC targeting agent [31].

The use of hybrid iron oxide-gold nanoparticles as a drug delivery system has additional practical advantages. Firstly, its gold shell is biocompatible and can easily be functionalised to attach various ligands including proteins like Cyt c. Secondly, due to its iron-oxide core it possesses with magnetic properties which could be used to direct magnetic nanoparticles to a desired location with the use of an external magnetic field. This allows the magnetic particles to accumulate at a much higher concentration in the area focused by the magnetic field, limiting the systemic effect on healthy tissues. Coating the gold shell of the particles with ligands that are highly specific in binding to receptors over-expressed on the tumor cell surface can further enhance the specificity of targeting therapeutic proteins. The magnetic properties also enable the visualisation of the nanoparticles by MRI enabling verification of their uptake in the desired anatomical location [32]. Hybrid iron oxide-gold nanoparticles also have the potential to bind doxorubicin as reported previously [33], thus the simultaneous delivery of doxorubicin and Cyt c can be achieved, which could further reduce the systemic undesired effects of the anticancer agent without compromising its clinical efficacy [34].

In summary, we report that very low dose of the pro-apoptotic Cyt c delivered into HepG2 cells significantly enhanced the efficacy of doxorubicin lowering its required concentration for the same effect on cell viability. The activation or inhibition of apoptotic pathway for therapeutic purposes is an area of intense research with significant potential benefits [35]. The synergistic effect of a pro-apoptotic protein and a cytotoxic anticancer agent could be exploited in practice, particularly in those areas of cancer therapy where conventional approaches have significant limitations.

Conclusion

Our results provide evidence that pro-apoptotic therapeutic protein delivery with hybrid nanoparticles complementing conventional anticancer drug administration is a feasible concept and further experiments are ongoing in our laboratory to enhance the efficacy of this method and optimize the application of pro-apoptotic proteins using a nano-sized drug delivery system.

Conflict of Interest

The authors would like to state that they have no conflict of interest with this work.

References

1. Pugalenti A, Cutter CS, Fong Y (2014) Current treatment for small (<5 cm) hepatocellular carcinoma: evolving roles for ablation and resection. *Adv Surg* 48: 97-114.
2. Murata S, Mine T, Sugihara F, Yasui D, Yamaguchi H, et al. (2014)

- Interventional treatment for unresectable hepatocellular carcinoma. *World J Gastroenterol* 20(37): 13453-13465.
- Watanabe K (2013) Current chemotherapeutic approaches for hepatoblastoma. *Int J Clin Oncol* 18(6): 955-961.
 - Tsimberidou AM, Letourneau K, Fu S, Hong D, Naing A, et al. (2011) Phase I clinical trial of hepatic arterial infusion of paclitaxel in patients with advanced cancer and dominant liver involvement. *Cancer Chemother Pharmacol* 68(1): 247-253.
 - Wilhelm SM, Adnane L, Newell P, Villanueva A, Llovet JM, et al. (2008) Preclinical overview of sorafenib, a multikinase inhibitor that targets both Raf and VEGF and PDGF receptor tyrosine kinase signaling. *Mol Cancer Ther* 7(10): 3129-3140.
 - Thomas MB (2014) Systemic and targeted therapy for biliary tract tumors and primary liver tumors. *Surg Oncol Clin N Am* 23(2): 369-381.
 - Zhang L, Zhou F, ten Dijke P (2013) Signaling interplay between transforming growth factor- β receptor and PI3K/AKT pathways in cancer. *Trends Biochem Sci* 38(12): 612-620.
 - Long JS, Ryan KM (2012) New frontiers in promoting tumor cell death: targeting apoptosis, necroptosis and autophagy. *Oncogene* 31(49): 5045-5060.
 - Martinou JC, Youle RJ (2011) Mitochondria in apoptosis: Bcl-2 family members and mitochondrial dynamics. *Dev Cell* 21(1): 92-101.
 - Sun F, Zhou Q, Pang X, Xu Y, Rao Z (2013) Revealing various coupling of electron transfer and proton pumping in mitochondrial respiratory chain. *Curr Opin Struct Biol* 23(4): 526-538.
 - Yuan S, Akey CW (2013) Apoptosome structure, assembly, and procaspase activation. *Structure* 21(4): 501-515.
 - Kim SK, Foote MB, Huang L (2012) The targeted intracellular delivery of Cytochrome C protein to tumors using lipid-apolipoprotein nanoparticles. *Biomaterials* 33(15): 3959-3966.
 - Liu G, Ma S, Li S, Cheng R, Meng F, et al. (2010) The highly efficient delivery of exogenous proteins into cells mediated by biodegradable chimaeric polymersomes. *Biomaterials* 31(29): 7575-7585.
 - Park HS, Kim CW, Lee HJ, Choi JH, Lee SG, et al. (2010) A mesoporous silica nanoparticle with charge-convertible pore walls for efficient intracellular protein delivery. *Nanotechnology* 21(22): 225101.
 - Li S, Meng F, Wang Z, Zhong Y, Zheng M, et al. (2012) Biodegradable polymersomes with an ionizable membrane: facile preparation, superior protein loading, and endosomal pH-responsive protein release. *Eur J Pharm Biopharm* 82(1): 103-111.
 - Santra S, Kaittanis C, Perez JM (2010) Cytochrome C encapsulating theranostic nanoparticles: a novel bifunctional system for targeted delivery of therapeutic membrane-impermeable proteins to tumors and imaging of cancer therapy. *Mol Pharm* 7(4): 1209-1222.
 - Morales-Cruz M, Figueroa CM, Gonzalez-Robles T, Delgado Y, Molina A, et al. (2014) Activation of caspase-dependent apoptosis by intracellular delivery of Cytochrome c-based nanoparticles. *J Nanobiotechnology* 12: 33.
 - Mendez J, Morales Cruz M, Delgado Y, Figueroa CM, Orellano EA, et al. (2014) Delivery of chemically glycosylated Cytochrome c immobilized in mesoporous silica nanoparticles induces apoptosis in HeLa cancer cells. *Mol Pharm* 11(1): 102-111.
 - Zwicke GL, Mansoori GA, Jeffery CJ (2012) Utilizing the folate receptor for active targeting of cancer nanotherapeutics. *Nano Rev* 3.
 - Xiang C, Zou Y, Qiu S, Sun L, Xu F, et al. (2013) Bionzymatic glucose biosensor based on direct electrochemistry of Cytochrome c on gold nanoparticles/polyaniline nanospheres composite. *Talanta* 110: 96-100.
 - Barnett C, Gueorguieva M, Lees MR, Darton R, McGarvey D, et al. (2012) The effect of the hybrid composition on the physicochemical properties and morphology of iron oxide-gold nanoparticles. *J Nano Res* 14: 1170.
 - Barnett C, Gueorguieva M, Lees MR, Darton R, McGarvey D, et al. (2013) Physical stability, biocompatibility and potential use of hybrid iron oxide-gold nanoparticles as drug carriers. *J Nano Res* 15: 1076.
 - Sharonov GV, Feofanov AV, Bocharova OV, Astapova MV, Dedukhova VI, et al. (2005) Comparative analysis of proapoptotic activity of Cytochrome c mutants in living cells. *Apoptosis* 10(4): 797-808.
 - Worns MA (2013) Systemic therapy and synergies by combination. *Dig Dis* 31(1): 104-111.
 - Rask-Andersen M, Zhang J, Fabbro D, Schioth HB (2014) Advances in kinase targeting: current clinical use and clinical trials. *Trends Pharmacol Sci pii: S0165-6147(14)00160-00166*.
 - Amaral JD, Xavier JM, Steer CJ, Rodrigues CM (2010) Targeting the p53 pathway of apoptosis. *Curr Pharm Des* 16(22): 2493-2503.
 - Manning MC, Chou DK, Murphy BM, Payne RW, Katayama DS (2010) Stability of protein pharmaceuticals: an update. *Pharm Res* 27(4): 544-575.
 - Aubin-Tam ME, Hwang W, Hamad-Schifferli K (2009) Site-directed nanoparticle labeling of Cytochrome c. *Proc Natl Acad Sci USA* 106(11): 4095-4100.
 - Aubin-Tam ME, Hamad-Schifferli K (2005) Gold nanoparticle-cytochrome C complexes: the effect of nanoparticle ligand charge on protein structure. *Langmuir* 21(26): 12080-12084.
 - Shang W, Nuffer JH, Muniz-Papandrea VA, Colon W, Siegel RW, et al. (2009) Cytochrome C on silica nanoparticles: influence of nanoparticle size on protein structure, stability and activity. *Small* 5(4): 470-476.
 - Joseph SC, Blackman BA, Kelly ML, Phillips M, Beaury MW, et al. (2014) Synthesis, characterization, and biological activity of poly (arginine)-derived cancer-targeting peptides in HepG2 liver cancer cells. *J Pept Sci* 20(9): 736-745.
 - Sensenig R, Sapir Y, MacDonald C, Cohen S, Polyak B (2012) Magnetic nanoparticle-based approaches to locally target therapy and enhance tissue regeneration *in vivo*. *Nanomedicine (Lond)* 7(9): 1425-1442.
 - Gautier J, Allard-Vannier E, Munnier E, Souce M, Chourpa I (2013) Recent advances in theranostic nanocarriers of doxorubicin based on iron oxide and gold nanoparticles. *J Control Release* 169(1-2): 48-61.
 - Li C, Li L, Keates AC (2012) Targeting cancer gene therapy with magnetic nanoparticles. *Oncotarget* 3(4): 365-370.
 - Hellebrand EE, Varbiro G (2010) Development of mitochondrial permeability transition inhibitory agents: a novel drug target. *Drug Discov Ther* 4(2): 54-61.